Photoinduced Electron-Transfer of Inclusion Complexes of Fullerenes (C_{60} and C_{70}) in γ-Cyclodextrin

Akito Masuhara, Mamoru Fujitsuka, and Osamu Ito*

Institute for Chemical Reaction Science, Tohoku University, Katahira, Aoba-ku, Sendai 980-8577

(Received January 27, 2000)

Photophysical and photochemical properties of 1 : 2 inclusion complexes of C_{60} and C_{70} in γ-cyclodextrin (γ-CD) have been studied by laser flash photolysis and steady photolysis methods. The triplet–triplet annihilations of C_{60}/γ-CD and C_{70}/γ-CD are retarded, compared with those of the pristine fullerenes. The rate constant for the fluorescence-quenching of C_{70}/γ-CD by 1,4-diazabicyclo[2.2.2]octane was larger than that of C_{60}/γ-CD, indicating incomplete hindrance by γ-CD due to larger size of C_{70} than C_{60}. A similar trend was also observed in triplet–triplet annihilation processes of the encapsulated fullerenes. Generations of radical ions by photoinduced electron transfer between amines and $^3C_{60}^*/\gamma$-CD or $^3C_{70}^*/\gamma$-CD were confirmed by observing the transient absorption bands due to radical anions in the near-IR region. The electron transfer rates for $^3C_{60}^*/\gamma$-CD or $^3C_{70}^*/\gamma$-CD were slower than those of corresponding $^3C_{60}^*$ or $^3C_{70}^*$ in solution by ca. 1/100. For reversible systems in which the cation radicals of amines are stable (for example, *p*-anisidine), $C_{60}^{\bullet-}/\gamma$-CD and $C_{70}^{\bullet-}/\gamma$-CD decayed slowly by back electron transfer. For an irreversible system in which the cation radical of amine (nitrilotriethanol) is degraded, the high concentration of $C_{60}^{\bullet-}/\gamma$-CD or $C_{70}^{\bullet-}/\gamma$-CD was persistent. On addition of methylviologen (MV^{2+}), persistent $MV^{\bullet+}$ was generated in high concentration as equilibrium with $C_{60}^{\bullet-}/\gamma$-CD, suggesting that C_{60}/γ-CD acts as an efficient photosensitizer and an electron mediator to produce $MV^{\bullet+}$ using nitrilotriethanol as a sacrificial donor.

Photoexcited fullerenes are good electron acceptors in the presence of electron donors such as amino compounds.[1—12] Since fullerenes are only soluble in organic solvents, studies of the photoinduced electron transfer reactions have been mainly carried out in organic solvents such as benzene and benzonitrile.[1—12] Several efforts have been devoted to dissolve fullerenes in aqueous media.[13—37] Although aqueous micellar solution dissolves C_{60}, the solubility is not high enough.[34—36] It has been reported that some host molecules such as γ-cyclodextrin (γ-CD) and calixarenes form inclusion complexes with fullerenes in aqueous solutions.[13—27] While the inclusion complex of C_{60} and calixarene in solution shows a brownish color due to CT interaction,[26,27] the inclusion complex of C_{60} in γ-CD (C_{60}/γ-CD) is purple pink, which is the characteristic color of the pristine C_{60} in organic solution, indicating small electronic interaction between the host and the guest. Water-soluble C_{60}/γ-CD can be applied to various photoinduced reactions in aqueous media; for example, C_{60}/γ-CD is considered to be an important candidate for the bio-mimetic reactions with enzymes.[34—36] The inclusion complex, C_{60}/γ-CD, can be prepared by several methods. Yoshida et al. have reported that the purple crystal of C_{60}/γ-CD can be obtained by their preparation method, which includes reflux of two liquid phases of C_{60} and γ-CD.[16] Recently, the ball-milling method enables one to get stable C_{60}/γ-CD with higher solubility in aqueous media.[18] This mechanochemical method makes it possible to include C_{70} in γ-CD (C_{70}/γ-CD), too, although the stability and solubility are somewhat lower than those of C_{60}/γ-CD.

In the present paper, we report the results of laser flash photolysis studies of C_{60}/γ-CD and C_{70}/γ-CD revealing properties of triplet excited states and their roles in photoinduced electron transfer processes. Photoinduced processes in the singlet excited states were also examined by time-resolved fluorescence measurements. The effects of γ-CD on the reactivities of the photoexcited C_{60} and C_{70} are discussed. It has been shown that C_{60}/γ-CD and C_{70}/γ-CD act as photosensitizers and electron-mediators in the presence of amino compounds and methylviologen. In the reaction system, fullerenes pump up an electron from donor amines and transfer it to water-soluble methylviologen.

Experimental

Materials. C_{60} (purity 99.5%) and C_{70} (99%) were purchased from Terms Co. Inclusion complexes of C_{60} and C_{70} in γ-CD (Wako Pure Chemicals) were prepared by ball-milling for 12 h at room temperature. Aqueous solutions of C_{60}/γ-CD and C_{70}/γ-CD were filtered just before the measurements with a membrane filter (pore size = 0.2μm) in order to exclude fine brownish particles. Inclusion of C_{70} in γ-CD was confirmed by the induced circular dichroism spectrum on JASCO J-20. In order to observe the transient absorption spectra up to 1600 nm, D_2O was employed as a solvent for C_{70}/γ-CD. Other chemicals such as *p*-anisidine (PAD), 2,2′,2″-nitrilotriethanol (NTE), and 1,4-diazabicyclo[2.2.2]octane (DABCO) were the best grade available.

Measurements. The nanosecond time-resolved absorption spectra were measured using second-harmonic generation (532 nm) or third-harmonic generation (355 nm) of a Nd : YAG laser (Quanta-Ray GCR-130, fwhm 6 ns) as an excitation source. For the tran-

sient absorption spectra in the near-IR region (600—1600 nm), a Ge avalanche photodiode (APD) (Hamamatsu Photonics, B2834) was employed as a detector for monitoring light from a pulsed xenon flash lamp.[38] The long time scale phenomena up to millisecond-region were measured using an InGaAs-PIN photodiode (Hamamatsu Photonics, G5125-10) or a Si-APD (Hamamatsu Photonics, S5343) as a detector for monitoring light from a continuous Xe-lamp (150 W).[39] All the samples for the laser flash photolysis experiments were deaerated by argon bubbling for 15 min in a 1 cm quartz cell.

Picosecond time-resolved fluorescence spectra were measured by a single-photon counting method using second-harmonic generation (365 nm) of a Ti : sapphire laser (Spectra-Physics, Tsunami 3950-L2S, fwhm 1.5 ps) and a streakscope (Hamamatsu Photonics, C4334-01) as an excitation source and a detector, respectively.

Steady-state absorption and fluorescence spectra were recorded on a JASCO V-570 DS spectrophotometer and a Shimadzu RF-5300PC spectrofluorometer, respectively. Steady-state photolysis was performed with an Xe–Hg lamp equipped with a sharp cut-off filter ($\lambda > 500$ nm).

Results and Discussion

Absorption Spectra of C_{60}/γ-CD and C_{70}/γ-CD. Steady-state absorption spectra of aqueous solutions of C_{60}/γ-CD and C_{70}/γ-CD show essentially the same spectral features as those of the pristine C_{60} and C_{70} in organic solvents, respectively (Fig. 1), indicating that γ-CD does not strongly affect the electronic nature of C_{60} and C_{70}. Thus, the concentrations of C_{60}/γ-CD and C_{70}/γ-CD were estimated using the reported molar extinction coefficients in organic solvent: C_{60} (1910 $dm^3\,mol^{-1}\,cm^{-1}$ at 407 nm) and C_{70} (14500 $dm^3\,mol^{-1}\,cm^{-1}$ at 468 nm).[40] The concentration of the typical sample solutions used for Fig. 1 is evaluated to be 1.0×10^{-4} mol dm^{-3}. In the case of C_{70}/γ-CD in H_2O and in D_2O, solubility and stability seem to be low compared with C_{60}/γ-CD; during argon bubbling, black precipitates appeared, which may be aggregated C_{70} ejected from γ-CD. The filtered aqueous solutions of C_{60}/γ-CD and C_{70}/γ-CD were quite stable for the laser irradiation, since absorption spectra after laser irradiation were the same as those before the irradiation.

Fluorescence of C_{60}/γ-CD and C_{70}/γ-CD. In Fig. 1, fluorescence spectra of C_{60}/γ-CD and C_{70}/γ-CD in aqueous solution are shown with those of the pristine fullerenes in benzene at the same concentration (1.0×10^{-4} mol dm^{-3}). The shapes of the fluorescence bands of C_{60}/γ-CD and C_{70}/γ-CD are essentially the same as those of the pristine C_{60} and C_{70} in benzene.[41—43] Fluorescence intensities of C_{60}/γ-CD and C_{70}/γ-CD seem to be slightly weaker than those of the pristine fullerenes. Fluorescence quantum yields (Φ_F) and lifetimes (τ_F) are estimated as shown in Table 1. The fluorescence lifetimes and peak positions are not changed by inclusion. The Φ_F values of the inclusion complexes are about half of those of the pristine fullerenes; although it is difficult to compare the variation of small absolute Φ_F values, the smaller Φ_F values of C_{60}/γ-CD and C_{70}/γ-CD may be related to the structural strain of fullerene molecules induced by the encapsulation in γ-CD.

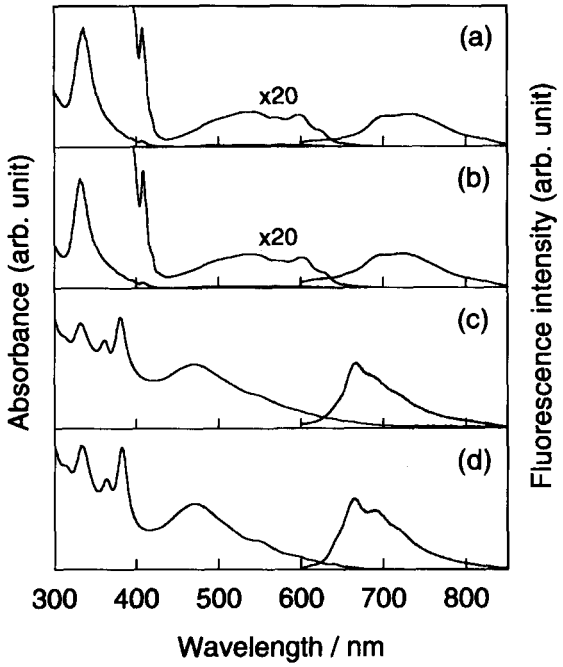

Fig. 1. Steady-state absorption spectra and fluorescence spectra in the UV/vis region: (a) C_{60}/γ-CD in water, (b) C_{60} in benzene, (c) C_{70}/γ-CD in water, and (d) C_{70} in benzene. Concentrations of fullerenes are 1.0×10^{-4} mol dm^{-3}.

On addition of amines such as DABCO, the decay rate of fluorescence intensity increases as shown in Fig. 2. The

Table 1. Properties of Singlet and Triplet Excited States of C_{60} and C_{70} in Benzene (Bz) and in γ-CD/H_2O or D_2O

	C_{60}/γ-CD/H_2O	C_{60}/Bz	C_{70}/γ-CD/D_2O	C_{70}/Bz
Singlet				
λ_A/nm[a)]	407	407	471	471
λ_F/nm[b)]	728	723	664	668
Φ_F	2×10^{-4}	3×10^{-4}	3×10^{-4}	7×10^{-4}
τ_F/ns	1.07	1.19	0.58	0.61
k_q^S/$dm^3\,mol^{-1}\,s^{-1}$	1.8×10^8	5.4×10^9	1.0×10^9	5.9×10^9
Triplet				
λ_T/nm[c)]	750	750	980	980
τ_T/μs	108	22	60	16
k_{TT}/$dm^3\,mol^{-1}\,s^{-1}$	1.7×10^8	1.1×10^9	7.5×10^8	3.4×10^9

a) Absorption maximum. b) Fluorescence maximum. c) Maximum of T–T absorption.

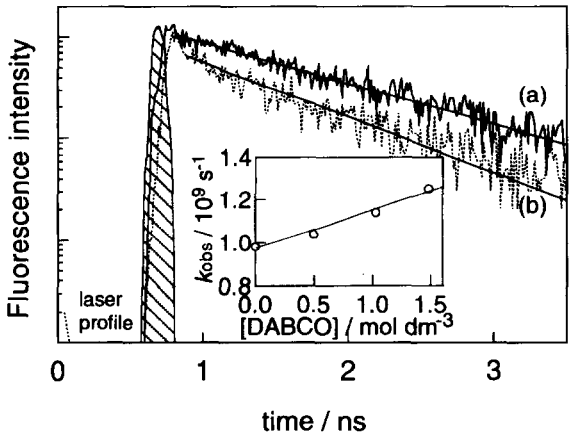

Fig. 2. Fluorescence-time profiles at 730 nm of C_{60}/γ-CD in H_2O (a) in the absence and (b) in the presence of 1.0 mol dm^{-3} of DABCO. Inset: Dependence of first-order rate on the concentration of DABCO.

increase in the decay rate can be attributed to the bimolecular processes including electron transfer via the singlet excited state of C_{60}/γ-CD. From the slopes of the first-order plots (inset of Fig. 2), the bimolecular quenching rate constants (k_q^S) were evaluated as listed in Table 1. The k_q^S for C_{60}/γ-CD is 1/30 of that for C_{60} in benzene. The observed k_q^S for C_{60}/γ-CD is 1/41 of the diffusion limiting rate of H_2O (k_{diff} = 7.4×10^9 dm^3 mol^{-1} s^{-1}).[44] These findings indicate inefficient fluorescence quenching due to steric hindrance by γ-CD surrounding C_{60}. In the case of C_{70}/γ-CD, the k_q^S value was 1/5.9 of that of C_{70} in benzene. The observed k_q^S value for C_{70}/γ-CD is larger than that of C_{60}/γ-CD probably indicating incomplete hindrance by γ-CD due to the size of C_{70} being larger than that of C_{60}.

Triplet Excited States of C_{60}/γ-CD and C_{70}/γ-CD. Laser irradiation of an aqueous solution of C_{60}/γ-CD generates an intense transient absorption band at 750 nm, as shown in Fig. 3. The transient absorption band can be attributed to the triplet excited state of C_{60}/γ-CD ($^3C_{60}^*/\gamma$-CD).[2,45] The peak position is almost the same as that of the pristine C_{60} excited in benzene. Similarly, the transient absorption band of the triplet excited state of C_{70}/γ-CD ($^3C_{70}^*/\gamma$-CD) was observed at 980 nm, which is the same peak position as $^3C_{70}^*$ in benzene.[43,46,47] The decay-time profile of the transient absorption band of $^3C_{60}^*/\gamma$-CD is shown in inset of Fig. 3. In order to estimate the triplet lifetime of fullerenes, the laser power dependence on the decay kinetics was examined.

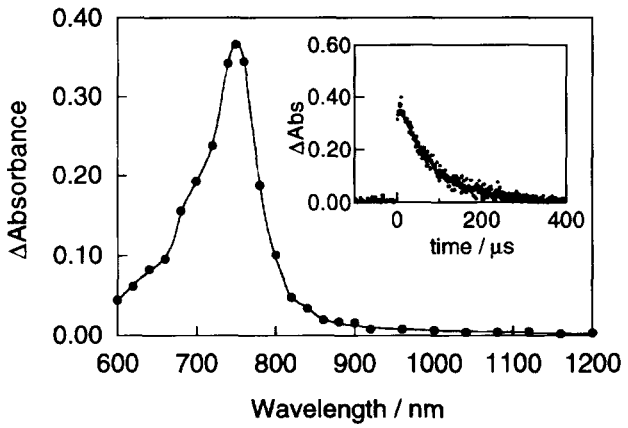

Fig. 3. Transient absorption spectrum of C_{60}/γ-CD (1.0×10^{-4} mol dm^{-3}) in deaerated water at 100 ns after 355 nm-laser irradiation. Inset: Absorption-time profile at 750 nm.

On increasing the laser power, the decay curves of the sample solution (1.0×10^{-4} mol dm^{-3}) changed to the mixed-order kinetics of the first- and the second-order, as shown in Fig. 4. For $^3C_{60}^*/\gamma$-CD, the half-life for the decay observed by the lowest laser power seems to be ca. 100 μs, whereas the half-life of the pristine $^3C_{60}^*$ seems to be ca. 20 μs.

For more quantitative treatment, the first-order rate constant (k_{1st}) and the second-order rate constant (k_{2nd}) were separated by using the following equation:[48,49]

$$-\mathrm{d}[\ln(\Delta A_0)]/\mathrm{d}t = \Delta k_{1st} = k_{1st}^0 + (2k_{2nd}/\varepsilon_T)\Delta A_0, \quad (1)$$

where ΔA_0, k_{1st}^0, and ε_T are T–T absorbance at $t = 0$, an intrinsic first-order decay rate, and an extinction coefficient of the T–T absorption band, respectively. In Fig. 4, the plots for $^3C_{60}^*/\gamma$-CD in aqueous solution and $^3C_{60}^*$ in benzene are shown as inserted figures.

From the slope, $2k_{2nd}$ can be evaluated as a ratio of ε_T. In the present case, the T–T annihilation (Eq. 2) is the most probable process for the second-order reaction.

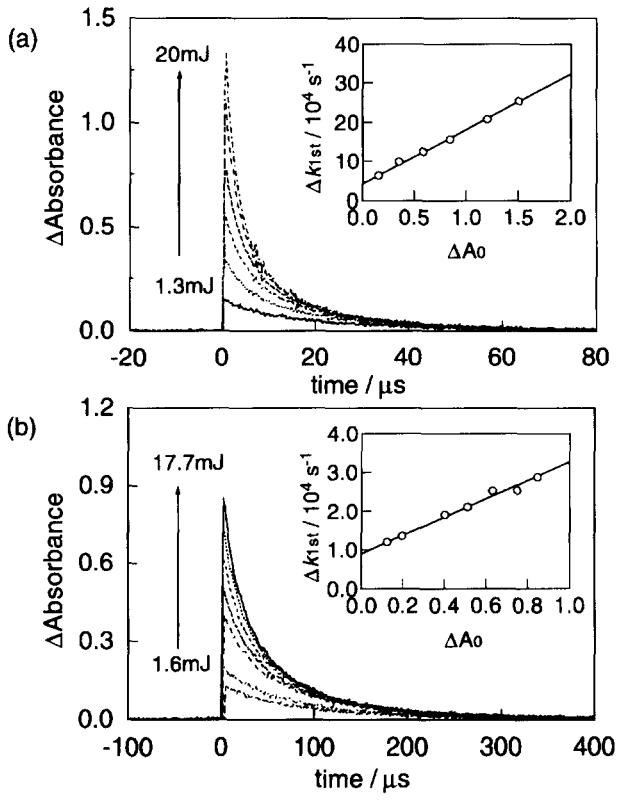

Fig. 4. Time profiles at 750 nm after 355 nm-laser irradiation. (a) C_{60} in deaerated benzene. (b) C_{60}/γ-CD (1.0×10^{-4} mol dm^{-3}) in deaerated water. Inset: Plots of Eq. 1 for C_{60} and C_{60}/γ-CD.

$$^3C_n^*/\gamma\text{-CD} + {}^3C_n^*/\gamma\text{-CD} \xrightarrow{k_{TT}} {}^1C_n^*/\gamma\text{-CD} + C_n/\gamma\text{-CD}, \quad n = 60, 70 \qquad (2)$$

where k_{TT} is the rate constant for the T–T annihilation. Thus, the fact that the slope for $^3C_{60}^*$ is steeper than that of $^3C_{60}^*/\gamma$-CD indicates larger k_{TT} value (Table 1). The k_{TT} values for $^3C_{60}^*$ and $^3C_{70}^*$ in benzene are 1/9.1 and 1/2.9 of the diffusion-controlled limit ($k_{diff} = 1.1\times10^{10}$ dm^3 mol^{-1} s^{-1}),[44] respectively, whereas k_{TT} values of $^3C_{60}^*/\gamma$-CD and $^3C_{70}^*/\gamma$-CD are 1/38 and 1/8.7 of k_{diff} in H_2O. These findings imply that T–T annihilation over the γ-CD capsule is retarded slightly, but not hindered completely. It is interesting to note that a k_{TT} of $^3C_{70}^*/\gamma$-CD slightly larger than that of $^3C_{60}^*/\gamma$-CD is the same trend as that observed in the k_q^S values of the encapsulated fullerenes.

The intercept of the inset of Fig. 4 gives k_{1st}^0, which is reciprocal of the intrinsic lifetime of the triplet state (τ_T). The smaller intercept of $^3C_{60}^*/\gamma$-CD gives a longer τ_T than the larger intercept of $^3C_{60}^*$ in benzene (Table 1). It is worth mentioning that the τ_T values of $^3C_{60}^*/\gamma$-CD and $^3C_{70}^*/\gamma$-CD are considerably longer compared with those of C_{60} and C_{70} in organic solutions, respectively. These findings indicate retardation of self-quenching process by capsulation in γ-CD.[50,51]

Photoinduced Electron Transfer. By the 355 nm-laser irradiation of C_{60}/γ-CD in the presence of PAD, a new absorption band appeared at 1080 nm with a decrease of the absorption band of $^3C_{60}^*/\gamma$-CD at 750 nm (Fig. 5 and its inset). The new absorption band at 1080 nm can be attributed to the radical anion of C_{60}/γ-CD ($C_{60}^{\bullet-}/\gamma$-CD), since the peak position is in good agreement with the reported position of $C_{60}^{\bullet-}$.[1,52] Since the decay rate of $^3C_{60}^*/\gamma$-CD (7.2×10^6 s^{-1}) is almost the same as the rise rate of $C_{60}^{\bullet-}/\gamma$-CD (7.6×10^6 s^{-1}) within the experimental error, the generation of $C_{60}^{\bullet-}/\gamma$-CD can be attributed to the electron transfer from PAD to $^3C_{60}^*/\gamma$-CD.

By the excitation of C_{70}/γ-CD with the 355 nm-laser pulse

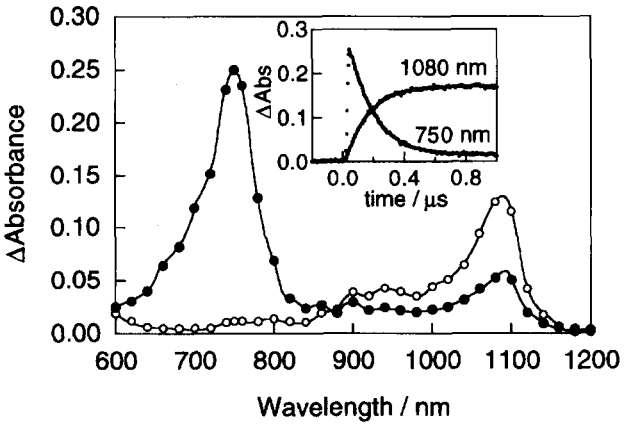

Fig. 5. Transient absorption spectra of C_{60}/γ-CD (1.0×10^{-4} mol dm^{-3}) in deaerated water in the presence of PAD (1.0×10^{-2} mol dm^{-3}) at 50 ns (solid circle) and 500 ns (open circle) after 355 nm-laser irradiation. Inset: Absorption-time profiles at 750 and 1080 nm.

in the presence of PAD, a transient absorption band due to radical anion of C_{70}/γ-CD ($C_{70}^{\bullet-}/\gamma$-CD) appeared at 1380 nm[53] with decrease of $^3C_{70}^*/\gamma$-CD at 980 nm, indicating that electron transfer occurs via $^3C_{70}^*/\gamma$-CD (Fig. 6 and its inset).

From the dependence of the observed first-order decay rates of $^3C_{60}^*/\gamma$-CD and $^3C_{70}^*/\gamma$-CD on the concentration of PAD, bimolecular triplet quenching rate constants (k_q^T) were estimated as summarized in Table 2. The k_q^T values are in good agreement with the corresponding values estimated from the rise profiles of $C_{60}^{\bullet-}/\gamma$-CD and $C_{70}^{\bullet-}/\gamma$-CD. This finding supports the electron transfer mechanism via $^3C_{60}^*/\gamma$-CD and $^3C_{70}^*/\gamma$-CD. The estimated rate constants for the encapsulated fullerenes are one-order smaller than the corresponding k_q^T values of the pristine $^3C_{60}^*$ and $^3C_{70}^*$ in benzonitrile. Similar electron transfer processes were also confirmed with other amines such as DABCO and NTE, and the k_q^T values were evaluated as in Table 2.

The quantum yield of the electron transfer process (Φ_{et})

Table 2. Free Energy Changes (ΔG), Quenching Rates (k_q^T), Quantum Yields (Φ_{et}), Electron Transfer Rates (k_{et}^T), and Back Electron Transfer Rates (k_{bet}) for the Electron-Transfer Systems of Fullerenes (C_{60}, C_{70}, C_{60}/γ-CD, and C_{70}/γ-CD) and Amines

Fullerenes	Donor	Solvent	ΔG / kJ mol^{-1}	k_q^T [a]	Φ_{et}	k_{et}^T [a]	k_{bet} [a]
C_{60}/γ-CD	PAD	H_2O	−49.7	6.8×10^8	0.54	3.7×10^8	1.0×10^8
C_{60}	PAD	BN	−65.2	4.3×10^9	0.39	1.7×10^9	8.6×10^9
C_{60}/γ-CD	DABCO	H_2O	−48.9	9.6×10^7	0.35	3.4×10^7	5.8×10^8
C_{60}	DABCO	BN	−54.3	3.2×10^9	0.64	2.0×10^9	1.0×10^{10}
C_{60}/γ-CD	NTE	H_2O	−14.1	9.8×10^6	0.18	1.8×10^6	—[b]
C_{60}	NTE	BN	−19.5	4.8×10^7	0.33	1.6×10^7	—[b]
C_{70}/γ-CD	PAD	D_2O	−51.8	8.9×10^8	0.59	5.2×10^8	2.3×10^8
C_{70}	PAD	BN	−56.0	4.7×10^9	0.66	3.1×10^9	1.3×10^{10}
C_{70}/γ-CD	DABCO	D_2O	−50.0	1.5×10^6	0.68	1.0×10^6	4.9×10^8
C_{70}	DABCO	BN	−56.0	3.9×10^9	0.68	2.7×10^9	6.7×10^{10}
C_{70}/γ-CD	NTE	D_2O	−16.0	3.5×10^6	0.79	2.8×10^6	—[b]
C70	NTE	BN	−21.4	6.1×10^7	0.51	3.1×10^7	—[b]

a) in dm^3 mol^{-1} s^{-1}. b) Back electron transfer was not observed.

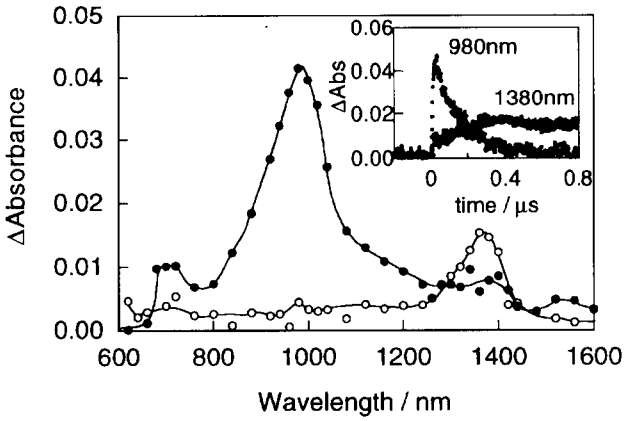

Fig. 6. Transient absorption spectra of C_{70}/γ-CD (1.0×10^{-4} mol dm^{-3}) in deaerated D_2O in the presence of PAD (1.0×10^{-2} mol dm^{-3}) at 50 ns (solid circle) and 500 ns (open circle) after 355 nm-laser irradiation. Inset: Absorption-time profiles at 980 and 1380 nm.

via the triplet state of fullerene was evaluated from the ratio of the maximal concentration of $C_{60}^{\bullet-}/\gamma$-CD to the initial concentration of $^3C_{60}^*/\gamma$-CD using the reported extinction coefficients of $C_{60}^{\bullet-}$ and $^3C_{60}^*$.[2,54] When the concentration of amine is high enough, the Φ_{et} takes a constant value (see next paragraph). The Φ_{et} values were estimated for $^3C_{60}^*/\gamma$-CD and $^3C_{70}^*/\gamma$-CD toward aromatic and aliphatic amines as listed in Table 2. The Φ_{et} values less than unity suggest that there are some deactivation processes other than the electron transfer (Eq. 3). Collisional deactivation in an encounter complex and quick back electron transfer within a geminate ion pair are the candidates for the quenching processes of the triplet state. In the present case, triplet energy transfer can be excluded from the possible pathways, because the triplet energies of C_{60} and C_{70} are low compared with the amines in this study.

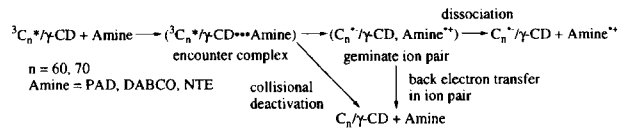

(3)

The Φ_{et} value depends on the concentration of amine as given in Eq. 4:

$$\Phi_{et} = k_{et}^T[\text{Amine}]/\{k_T^0 + k_q^T[\text{Amine}]\}, \quad (4)$$

where k_T^0 and k_{et}^T are the decay rate of C_n/γ-CD without amine and the rate constant for the electron transfer, respectively. When $k_T^0 \ll k_q^T$ [Amine], the k_{et}^T value can be obtained from the following equation: $k_{et}^T = k_q^T \times \Phi_{et}$.[55] Thus, the k_{et}^T values of $^3C_{60}^*/\gamma$-CD and $^3C_{70}^*/\gamma$-CD were evaluated as listed in Table 2. The k_{et}^T values in benzonitrile for PAD ($E_{ox} = 0.56$ V) and DABCO (0.57 V) are larger than those for NTE ($E_{ox} = 0.93$ V). The observed tendency can be well explained on the basis of the free energy change of electron transfer (ΔG) calculated using Rehm–Weller equation (Table 2).[56] Larger k_{et}^T values are observed with the reaction systems with negatively larger ΔG values.

For aromatic amine (PAD) and aliphatic amine (NTE), the k_{et}^T values of $^3C_{60}^*/\gamma$-CD and $^3C_{70}^*/\gamma$-CD are smaller than those for the pristine $^3C_{60}^*$ and $^3C_{70}^*$ in benzonitrile by a factor of ca. 1/10. On the other hand, for DABCO, the k_{et}^T values of $^3C_{60}^*/\gamma$-CD and $^3C_{70}^*/\gamma$-CD are smaller than those for $^3C_{60}^*$ and $^3C_{70}^*$ in benzonitrile by a factor of ca. 1/100. The ΔG values of the encapsulated fullerenes in H_2O/D_2O (Table 2), which were estimated by the Weller equation,[57] are similar values to those of the pristine fullerenes in benzonitrile. From these ΔG values, the observed large differences of k_{et}^T values in the ranges of 1/10—1/100 can not be explained. Thus, the small k_{et}^T values of γ-CD-encapsulated fullerenes indicate that the electron-transfer processes between fullerenes and amines are retarded by γ-CD surrounding fullerenes, because the electron transfer rate depends on the distance largely.[58] These findings suggest that the forward electron transfer occurs efficiently only when donor and acceptor are close each other.

Back Electron Transfer. For donors such as PAD and DABCO, the generated radical anions disappear over several hundred microseconds, as shown in the inset of Fig. 7, after reaching the maximal concentration at ca. 5 μs after the laser excitation. The observed time-profiles were analyzed by second-order plots as in Fig. 7. Since both electron transfer systems show good fits with linear lines of the second-order plots, the decay of $C_{60}^{\bullet-}/\gamma$-CD and $C_{60}^{\bullet-}$ may be mainly attributed to the back electron transfer reactions (Eq. 5):

$$C_n^{\bullet-}/\gamma\text{-CD} + \text{Amine}^{\bullet+} \xrightarrow{k_{bet}} C_n/\gamma\text{-CD} + \text{Amine}. \quad n = 60, 70 \quad (5)$$

From each slope ($= k_{bet}/\varepsilon_A$, where k_{bet} and ε_A are the rate constant of the back electron transfer process and the molar extinction coefficient of $C_{60}^{\bullet-}$, respectively), the k_{bet} value was evaluated by substituting the ε_A value. From the second-order plots in Fig. 7, it is evident that the slope of $C_{60}^{\bullet-}$ is steeper than that of $C_{60}^{\bullet-}/\gamma$-CD. This indicates that the k_{bet}

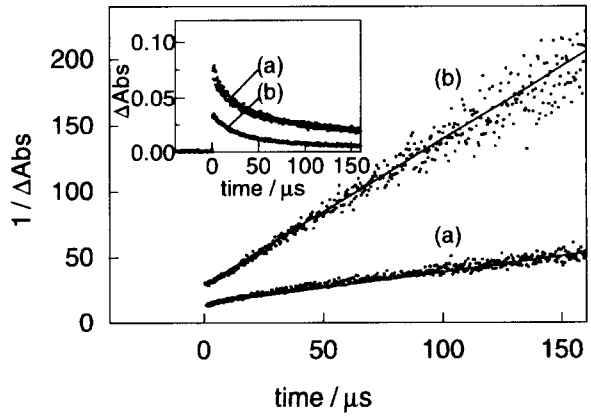

Fig. 7. Second-order plots at 1080 nm for absorption-time profiles (inset) observed after laser exposure of (a) C_{60}/γ-CD (1.0×10^{-4} mol dm^{-3}) in the presence of DABCO (1.0×10^{-2} mol dm^{-3}) in deaerated water and (b) C_{60} (1.0×10^{-4} mol dm^{-3}) in the presence of DABCO (5.0×10^{-3} mol dm^{-3}) in deaerated benzonitrile.

value of $C_{60}^{\bullet-}$ is much larger than that of $C_{60}^{\bullet-}/\gamma$-CD. The estimated k_{bet} values are summarized in Table 2 including the k_{bet} values for $C_{70}^{\bullet-}/\gamma$-CD and $C_{70}^{\bullet-}$ evaluated similarly. It should be noted that the k_{bet} values for $C_{60}^{\bullet-}$ and $C_{70}^{\bullet-}$ are close to k_{diff}. On the other hand, the k_{bet} values for $C_{60}^{\bullet-}/\gamma$-CD and $C_{70}^{\bullet-}/\gamma$-CD are one-order smaller than those of corresponding fullerene anions, indicating that γ-CD acts as a retarder for the back electron transfer, too.

In the case of NTE, high steady-concentrations of $C_{60}^{\bullet-}$ and $C_{70}^{\bullet-}$ were observed for both encapsulated and the pristine fullerenes, after the laser irradiation. Figure 8 shows the steady-state absorption spectra observed by steady-state photolysis of C_{60}/γ-CD in the presence of NTE. The absorption bands of $C_{60}^{\bullet-}$ increased with the photolysis (inset of Fig. 8). By the photolysis for 5 min, all the fed C_{60}/γ-CD was converted to $C_{60}^{\bullet-}/\gamma$-CD. The same spectral change was also observed with the reaction between C_{60} (or C_{70}) and NTE in benzonitrile. These findings indicate that the back electron transfer reaction between $C_{60}^{\bullet-}$ and $NTE^{\bullet+}$ was suppressed, because of the degradation reactions of $NTE^{\bullet+}$ before the back electron transfer.[59]

Photosensitized Reduction of MV^{2+}. Long-lived $C_{60}^{\bullet-}/\gamma$-CD is useful in wide applications to further reactions. Here, as an example, reduction of methylviologen (MV^{2+}) by $C_{60}^{\bullet-}/\gamma$-CD was attempted. In the steady-state photolysis of C_{60}/γ-CD in the presence of NTE and MV^{2+}, the absorption band of $MV^{\bullet+}$ appeared around 600 nm (Fig. 9), accompanying the absorption band of $C_{60}^{\bullet-}/\gamma$-CD, which is quite weak compared with that in Fig. 8. $MV^{\bullet+}$ may be produced by the electron transfer from $C_{60}^{\bullet-}/\gamma$-CD to MV^{2+}. Since both the anion radical and cation radical are present in the same solution, $C_{60}^{\bullet-}/\gamma$-CD and $MV^{\bullet+}$ are present in equilibrium. The equilibrium constant (K_M) was calculated to be 1.3×10^{-3} from the inserted difference spectrum in Fig. 9. This finding suggests that equal amounts of $C_{60}^{\bullet-}/\gamma$-CD and $MV^{\bullet+}$ are present when $[MV^{2+}] = 770\ [C_{60}/\gamma\text{-CD}]$.

In order to confirm electron transfer from $C_{60}^{\bullet-}/\gamma$-CD to

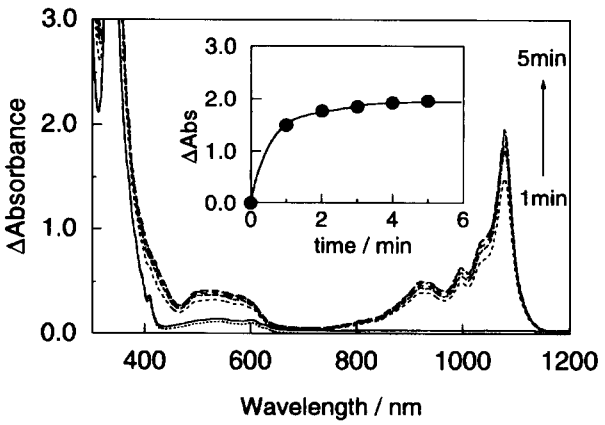

Fig. 8. Steady-state absorption spectra observed by photolysis of aqueous solution of C_{60}/γ-CD (1.0×10^{-4} mol dm^{-3}) in the presence of NTE (1.0×10^{-1} mol dm^{-3}) with a Xe–Hg lamp equipped with a sharp cut filter (> 500 nm). Inset: Absorption–time profile at 1080 nm.

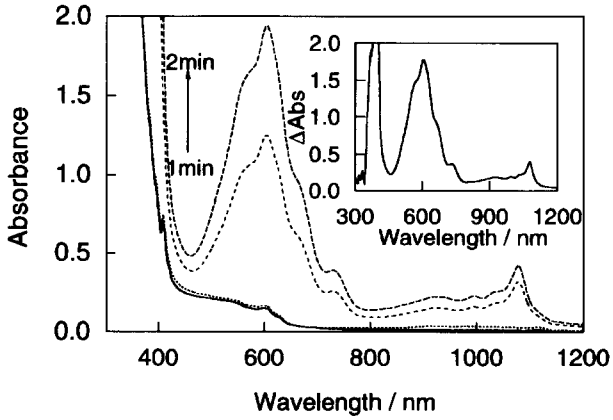

Fig. 9. Steady-state absorption spectra observed by photolysis of aqueous solution of C_{60}/γ-CD (1.0×10^{-4} mol dm^{-3}) in the presence of NTE (1.0×10^{-1} mol dm^{-3}) and MV^{2+} (2.0×10^{-1} mol dm^{-3}) with a Xe–Hg lamp equipped with a sharp cut filter (> 500 nm). Inset: Difference spectrum.

MV^{2+}, the laser photolysis experiment was performed for C_{60}/γ-CD in the presence of NTE and MV^{2+}. The generation of $MV^{\bullet+}$ at 600 nm was observed with the decay of $C_{60}^{\bullet-}/\gamma$-CD at 1080 nm (Fig. 10). The finding indicates that C_{60} pumps up an electron from NTE and donates the electron to MV^{2+}, as shown in Eq. 6.

$$\begin{array}{l} {}^3C_n{}^*/\gamma\text{-CD} + \text{Amine} \xrightarrow{k_{et}} C_n{}^{\bullet-}/\gamma\text{-CD} + \text{Amine}^{\bullet+} \\ \qquad\qquad\qquad\qquad\qquad\qquad\quad + MV^{2+} \quad \searrow k_{deg} \\ \text{n = 60, 70} \\ \text{Amine = NTE} \qquad\qquad\qquad\quad k_{-M} \uparrow\downarrow k_M \\ \qquad\qquad\qquad\qquad\quad C_n/\gamma\text{-CD} + MV^{\bullet+} \end{array} \tag{6}$$

From the rise of $MV^{\bullet+}$ and decay of $C_{60}^{\bullet-}/\gamma$-CD, the electron transfer rate (k_M) in Eq. 6 was estimated to be 4.3×10^6 dm^3 mol^{-1} s^{-1}. Thus, k_{-M} can be calculated to be 3.3×10^9 dm^3 mol^{-1} s^{-1} from the observed K_M. This suggests that the electron acceptor-ability of C_{60}/γ-CD is higher than MV^{2+} in aqueous solution. The finding is supported by the reduction

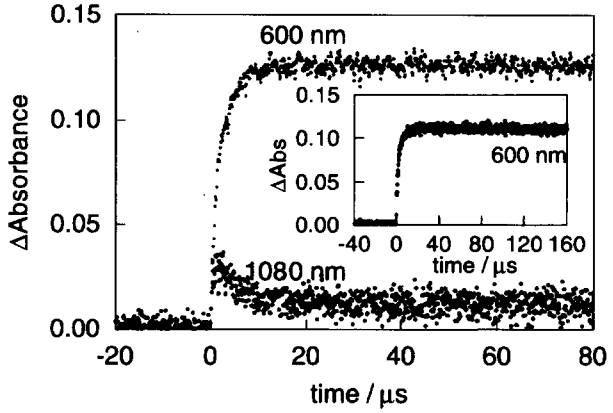

Fig. 10. Absorption–time profiles of $MV^{\bullet+}$ (600 nm) and $C_{60}^{\bullet-}/\gamma$-CD (1080 nm) observed by 355 nm-laser photolysis of C_{60}/γ-CD (1.0×10^{-4} mol dm^{-3}) in the presence of NTE (1.0×10^{-1} mol dm^{-3}) and MV^{2+} (2.0×10^{-1} mol dm^{-3}) in deaerated water. Inset: Absorption–time profile at 600 nm in long time-scale.

potentials of C_{60} and MV^{2+}, which are reported to be −0.42 and −0.45 V vs. SCE, respectively, in polar media.[1,58] Even by long time scale measurement (inset of Fig. 10), $MV^{\bullet+}$ does not show any decay. The absorption-time profile of $C_{60}^{\bullet-}/\gamma$-CD also shows a non-decaying part. The finding is in good agreement with the steady-state observation of $C_{60}^{\bullet-}/\gamma$-CD as equilibrium with $MV^{\bullet+}$. These observations indicate that $C_{60}^{\bullet-}/\gamma$-CD acts as an efficient photosensitizer for the persistent $MV^{\bullet+}$ formation using NTE as a sacrificial electron donor.

In the steady-state photolysis of C_{60}/γ-CD in the presence of DABCO and MV^{2+} (Fig. 11), the accumulation of $MV^{\bullet+}$ and $C_{60}^{\bullet-}/\gamma$-CD was also observed, but the absorption bands are broader and the concentrations are lower than those of the reaction with NTE. The decay of $C_{60}^{\bullet-}/\gamma$-CD and the rise of $MV^{\bullet+}$ in the laser photolysis experiments (Fig. 12) indicate that the electron-mediating role of C_{60} is similar to that in the reaction with NTE. After reaching maximal concentration around 5 μs, $MV^{\bullet+}$ begins to decay. This decrease in the concentration of $MV^{\bullet+}$ indicates that the electron transfer equilibrium between $C_{60}^{\bullet-}/\gamma$-CD and $MV^{\bullet+}$ is competitive with the back electron transfer between $C_{60}^{\bullet-}/\gamma$-CD and $DABCO^{\bullet+}$ (Eq. 7).

$$^3C_n^*/\gamma\text{-CD} + \text{Amine} \xrightarrow{k_{et}} C_n^{\bullet-}/\gamma\text{-CD} + \text{Amine}^{\bullet+} \xrightarrow{k_{bet}} C_n/\gamma\text{-CD} + \text{Amine}$$

$$\text{n = 60, 70} \qquad \uparrow\downarrow + MV^{2+}$$

$$\text{Amine = PAD, DABCO} \quad k_{-M} \uparrow\downarrow k_M$$

$$C_n/\gamma\text{-CD} + MV^{\bullet+} \qquad (7)$$

The generated $MV^{\bullet+}$ decays down to a low concentration, as shown in long time scale decay-profile (inset of Fig. 12), which is similar to the long-time decay of $C_{60}^{\bullet-}/\gamma$-CD shown in Fig. 7. The decay of $MV^{\bullet+}$ obeys the second-order kinetics, giving the back electron transfer rate constant, 5.0×10^8 $dm^3\ mol^{-1}\ s^{-1}$, which is similar to the k_{bet} value of $C_{60}^{\bullet-}/\gamma$-CD and $DABCO^{\bullet+}$.

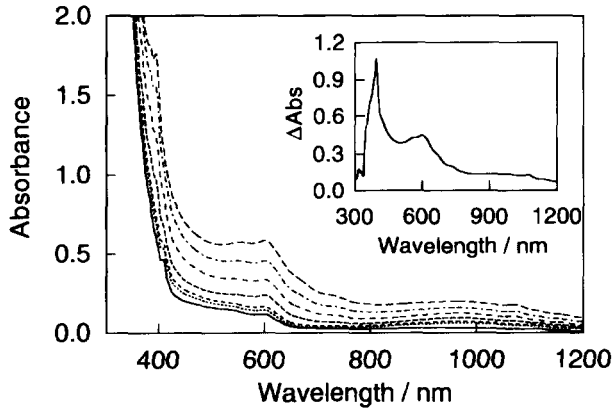

Fig. 11. Steady-state absorption spectra observed by photolysis of aqueous solution of C_{60}/γ-CD (1.0×10^{-4} mol dm^{-3}) in the presence of DABCO (5.0×10^{-2} mol dm^{-3}) and MV^{2+} (2.0×10^{-1} mol dm^{-3}) with a Xe–Hg lamp equipped with a sharp cut filter (> 500 nm). Inset: Difference spectrum.

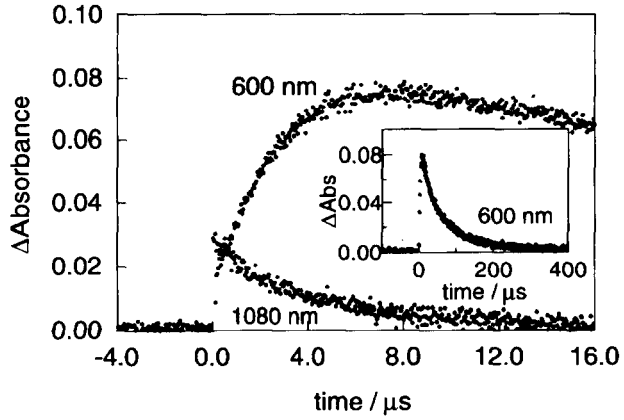

Fig. 12. Absorption–time profiles of $MV^{\bullet+}$ (600 nm) and $C_{60}^{\bullet-}/\gamma$-CD (1080 nm) observed by 355 nm-laser photolysis of C_{60}/γ-CD (1.0×10^{-4} mol dm^{-3}) in the presence of DABCO (5.0×10^{-2} mol dm^{-3}) and MV^{2+} (2.0×10^{-1} mol dm^{-3}) in water. Inset: Absorption–time profile at 600 nm in long time-scale.

Concluding Remarks

Photophysical properties of C_{60}/γ-CD and C_{70}/γ-CD are quite similar to those of C_{60} and C_{70} in organic solvents. However, bimolecular reactions such as electron and energy transfer processes of C_{60} and C_{70} are influenced by encapsulation in γ-CD. It has been revealed that γ-CD acts as a retarder in these bimolecular reactions. Furthermore, encapsulation in γ-CD enables one to study photochemistry of fullerenes in water media. It was found in water media that C_{60}/γ-CD acts as an efficient photosensitizer and an electron mediator to generate persistent $MV^{\bullet+}$. This reaction enables us to construct a novel catalytic reaction cycle using fullerenes.

The present work was partly supported by Grants-in-Aid on Scientific Research No. 10207202, 11740380, and 12875163 from the Ministry of Education, Science, Sports and Culture. The authors are also grateful to financial support by Core Research for Evolutional Science and Technology (CREST) of Japan Science and Technology Corporation.

References

1 J. W. Arbogast, C. S. Foote, and M. Kao, *J. Am. Chem. Soc.*, **114**, 2277 (1992).

2 L. Biczok, H. Linschitz, and R. I. Walter, *Chem. Phys. Lett.*, **195**, 339 (1992).

3 D. K. Palit, H. N. Ghosh, H. Pal, A. V. Sapre, J. P. Mittal, R. Seshadri, and C. N. R. Rao, *Chem. Phys. Lett.*, **198**, 113 (1992).

4 H. N. Ghosh, H. Pal, A. V. Sapre, and J. P. Mittal, *J. Am. Chem. Soc.*, **115**, 11722 (1993).

5 Y. Kajii, K. Takeda, and K. Shibuya, *Chem. Phys. Lett.*, **204**, 283 (1993).

6 Y. -P. Sun, C. E. Bunker, and B. Ma, *J. Am. Chem. Soc.*, **116**, 9692 (1994).

7 Y. -P. Sun, B. Ma, and G. E. Lawson, *Chem. Phys. Lett.*, **233**, 57 (1995).

8 J. V. Casper and Y. Wang, *Chem. Phys. Lett.*, **218**, 221 (1994).
9 B. Ma, G. E. Lawson, C. E. Bunker, A. Kitaygorodskiy, and Y. -P. Sun, *Chem. Phys. Lett.*, **247**, 51 (1995).
10 O. Ito, Y. Sasaki, Y. Yoshikawa, and A. Watanabe, *J. Phys. Chem.*, **99**, 9838 (1995).
11 M. Fujitsuka, A. Watanabe, O. Ito, K. Yamamoto, and H. Funasaka, *J. Phys. Chem. A*, **101**, 4840 (1997).
12 M. Fujitsuka, C. Luo, and O. Ito, *J. Phys. Chem. B*, **103**, 445 (1999).
13 T. Andersson, K. Nilsson, M. Sundahl, G. Westman, and O. Wennerstrom, *J. Chem. Soc., Chem.Commun.*, **1992**, 604.
14 N. M. Dimitrijevic and P. V. Kamat, *J. Phys. Chem.*, **97**, 7623 (1993).
15 D. M. Guldi, H. Hungerbuhler, E. Janata, and K. -D. Asmus, *J. Phys. Chem.*, **97**, 11258 (1993).
16 Z. Yoshida, H. Takekuma, S. Takekuma, and Y. Matsubara, *Angew. Chem., Int. Ed. Engl.*, **33**, 1597 (1994).
17 T. Andersson, M. Sundahl, G. Westman, and O. Wennerström, *Tetrahedron Lett.*, **35**, 7103 (1994).
18 T. Braun, Á. B. Barcza, L. Barcza, I. K. Thege, M. Fodor, and B. Migali, *Solid State Ionics*, **74**, 47 (1994).
19 K. I. Priyadarsini, H. Mohan, A. K. Tyagi, and J. P. Mittal, *Chem. Phys. Lett.*, **230**, 317 (1994).
20 K. I. Priyadarsini, H. Mohan, A. K. Tyagi, and J. P. Mittal, *J. Phys. Chem.*, **98**, 4756 (1994).
21 K. I. Priyadarsini, H. Mohan, J. P. Mittal, D. M. Guldi, and K. -D. Asmus, *J. Phys. Chem.*, **98**, 9565 (1994).
22 D. M. Guldi, H. Hunderbühler, and K. -D. Asmus, "Fullerenes," *Electrochem. Soc. Proc.*, **94-24**, 854 (1994).
23 V. Ohlendorf, A. Willnow, H. Hungerbühler, D. M. Guldi, and K. -D. Asmus, *J. Chem. Soc., Chem. Commun.*, **1995**, 759.
24 K. I. Priyadarsin and H. Mohan, *J. Photochem. Photobiol. A: Chem.*, **85**, 63 (1995).
25 G. Marconi, B. Mayer, C. T. Klein, and G. Köhler, *Chem. Phys. Lett.*, **260**, 589 (1996).
26 R. M. Williams and J. W. Verhoeven, *Recl. Trav. Chim. Pays-Bas*, **111**, 531 (1992).
27 S. D. -M. Islam, M. Fujitsuka, O. Ito, A. Ikeda, T. Hatano, and S. Shinkai, *Chem. Lett.*, **2000**, 78.
28 H. Hungerbuhler, D. M. Guldi, and K. -D. Asmus, *J. Am. Chem. Soc.*, **115**, 3386 (1993).
29 D. M. Guldi, H. Hunderbühler, and K. -D. Asmus, *J. Phys. Chem. A*, **101**, 1783 (1997).
30 D. M. Guldi, *J. Phys. Chem. A*, **101**, 3895 (1997).
31 S. Takenaka, K. Yamashita, M. Takagi, T. Hatta, A. Tanaka, and O. Tsuge, *Chem. Lett.*, **1999**, 319.
32 S. Takenaka, K. Yamashita, M. Takagi, T. Hatta, A. Tanaka, and O. Tsuge, *Chem. Lett.*, **1999**, 321.
33 Y. N. Yamakoshi, T. Yagami, K. Fukuhara, S. Sueyoshi, and N. Miyata, *J. Chem. Soc., Chem. Commun.*, **1994**, 517.
34 T. Tsuchiya, Y. Yamakoshi, and N. Miyata, *Biochem. Biophys. Res. Commun.*, **206**, 885 (1995).
35 T. Tsuchiya, I. Oguri, Y. Yamakoshi, and N. Miyata, *Fullerene Sci. Technol.*, **4**, 989 (1996).
36 Y. Yamakoshi, S. Sueyoshi, K. Fukuhara, and N. Miyata, *J. Am. Chem. Soc.*, **120**, 12363 (1998).
37 H. Onodera, A. Masuhara, M. Fujitsuka, O. Ito, S. Higashida, H. Imahori, and Y. Sakata, *Chem. Lett.*, **2000**, 426.
38 A. Watanabe and O. Ito, *J. Phys. Chem.*, **98**, 7736 (1994).
39 T. Konishi, Y. Sasaki, M. Fujitsuka, Y. Toba, H. Moriyama, and O. Ito, *J. Chem. Soc., Perkin Trans. 2*, **1999**, 551.
40 P. -M. Allemand, A. Koch, F. Wudl, Y. Rubin, F. Diederich, M. M. Alvarez, S. J. Anz, and R. L. Whetten, *J. Am. Chem. Soc.*, **113**, 1050 (1991).
41 D. Kim, M. Lee, Y. D. Suh, and S. K. Kim, *J. Am. Chem. Soc.*, **112**, 4429 (1992).
42 A. Watanabe, O. Ito, and K. Mochida, *Organometallics*, **14**, 4281 (1995).
43 A. Watanabe, O. Ito, M. Watanabe, H. Saitoh, and M. Koishi, *J. Phys. Chem.*, **100**, 10518 (1995).
44 S. L. Murov, I. Carmichael, and G. L. Hug, "Handbook of Photochemistry," 2nd ed, Marcel Dekker, New York (1993).
45 J. W. Arbogast, A. P. Darmanyan, C. S. Foote, Y. Rubin, F. N. Diederich, M. M. Alvarez, S. J. Anz, and R. L. Whetten, *J. Phys. Chem.*, **95**, 11 (1991).
46 J. W. Arbogast and C. S. Foote, *J. Am. Chem. Soc.*, **113**, 8886 (1991).
47 N. D. Dimitrijevic and P. V. Kamat, *J. Phys. Chem.*, **96**, 4811 (1992).
48 E. F. Zwicker and L. I. Grossweiner, *J. Phys. Chem.*, **67**, 549 (1963).
49 M. M. Alam, M. Fujitsuka, A. Watanabe, and O. Ito, *J. Phys. Chem.*, **102**, 1338 (1998).
50 M. R. Fraelich and R. B. Weisman, *J. Phys. Chem.*, **97**, 11145 (1993).
51 K. D. Ausman and R. B. Weisman, *Res. Chem. Intermed.*, **23**, 431 (1997).
52 T. Kato, T. Kodama, and T. Shida, *Chem. Phys. Lett.*, **205**, 405 (1993).
53 D. R. Lawson, D. L. Feldheim, C. A. Foss, P. K. Dorhout, C. M. Elliott, C. R. Martin, and B. Parkinson, *J. Phys. Chem.*, **96**, 7175 (1992).
54 G. A. Heath, J. E. McGrady, and R. L. Martin, *J. Chem. Soc., Chem. Commun.*, **1992**, 1272.
55 M. M. Alam, A. Watanabe, and O. Ito, *Bull. Chem. Soc. Jpn.*, **70**, 1833 (1997).
56 D. Rehm and A. Weller, *Isr. J. Chem.*, **8**, 259 (1970).
57 A. Weller, *Z. Phys. Chem. Neue Folge*, **133**, 93 (1982).
58 G. J. Karvarnos and N. J. Turro, *Chem. Rev.*, **86**, 401 (1986).
59 B. Ma, G. E. Lawson, C. E. Bunker, A. Kitaygorodskiy, and Y. -P. Sun, *Chem. Phys. Lett.*, **247**, 51 (1993).